JOURNAL OF PROPULSION AND POWER
Vol. 12, No. 3, May–June 1996

Aluminum Alloy Compatibility with Gelled Inhibited Red Fuming Nitric Acid

Michael F. A. Dove*
University of Nottingham, Nottingham NG7 2RD, England, United Kingdom
Norman Logan†
University of Alabama in Huntsville, Huntsville, Alabama 35899
Jeremy P. Mauger‡
University of Nottingham, Nottingham NG7 2RD, England, United Kingdom
Barry D. Allan§
Redstone Arsenal, Huntsville, Alabama 35898
and
Ramona E. Arndt¶ and Clark W. Hawk**
University of Alabama in Huntsville, Huntsville, Alabama 35899

Gelled inhibited red fuming nitric acid (IRFNA) is being considered as the oxidizer for advanced propulsion systems for the next generation U.S. Army missiles. The advanced systems have strict weight and volume limitations. Therefore, the desire is to use the strongest, lightest-weight materials for construction that are also compatible with the propellant ingredients. Aluminum alloys have traditionally been used to contain IRFNA. However, a minimum amount of quantitative corrosion rate data is available on the standard alloys, and less on the aluminum alloys being considered for advanced missile systems. This article provides data and information on the compatibility and corrosion rate of IRFNA gels of various compositions with several different aluminum alloys. Oxidizer composition changes included the addition of inhibitors such as P_4O_{10} to replace and/or supplement the hydrogen fluoride already present in the IRFNA. Low corrosion rates were obtained in certain gelled systems. Data were obtained by 1) electrochemical methods, 2) surface analytical methods, and 3) weight loss/change methods. The combination of methods provides useful data and is applicable to a variety of systems. The combined methods provide useful corrosion rates and long-term storage data for metals in contact with corrosive materials. The techniques and procedures are suitable for a variety of systems. The corrosion rate was found to decrease with time and stabilize quickly because of the formation of a protective film on the metal surface. The corrosion rates measured in neat IRFNA and gelled IRFNA were comparable.

Nomenclature

a = area exposed to oxidizer, cm^2
B = $b_a(-b_c)/2.303(b_a - b_c)$, V
b_a = anodic Tafel constant, V $decade^{-1}$
b_c = cathodic Tafel constant, V $decade^{-1}$
d = penetration depth into the metal or total corrosion of the metal, mil or μm
E_{corr} = rest potential, mV
F = Faraday, 96,484.6 C/mole
I_{corr} = corrosion current, A
ICR = instantaneous corrosion rate (electrochemistry), $mg/cm^2 \cdot day$
i_{corr} = corrosion current density, $A/m^2 \approx$ corrosion rate, mm/year
R = 8.31441 J K^{-1} mol^{-1}
R_p = polarization resistance, Ω
r^2 = least-squares-fit value
T = 298.15 K (25°C)
TACR = time-average corrosion rate (weight loss), $mg/cm^2 \cdot day$
W_e = waste equivalent of pure aluminum, 9 g/mole
z_a = $3(Al \rightarrow Al^{3+} + 3e^-)$
z_c = $1(NO_2^+ + e^- \rightarrow 1/2N_2O_4$ or $NO^+ + e^- \rightarrow NO)$
β = 0.5, symmetry factor or transmission coefficient
ρ = density of pure aluminum, 2.699 g/cm^3

Presented in part as Paper 94-3257 at the AIAA/ASME/SAE/ASEE 30th Joint Propulsion Conference and Exhibit, Indianapolis, IN, June 27–29, 1994; received Feb. 22, 1995; revision received Nov. 13, 1995; accepted for publication Nov. 13, 1995.

*Senior Lecturer, Department of Chemistry. Member AIAA.
†Visiting Scholar, Propulsion Research Center; currently University Research Fellow, Department of Chemistry, University of Nottingham, Nottingham NG7 2RD, England, UK. Member AIAA.
‡Graduate Student, Department of Chemistry; currently Examiner, European Patent Office, Munich, Germany.
§Group Leader, MICOM Propulsion Directorate, Advanced Propulsion.
¶Graduate Research Assistant. Student Member AIAA.
**Director, Propulsion Research Center, Professor, Department of Mechanical and Aerospace Engineering. Associate Fellow AIAA.

Introduction

A SERIES of inhibited red fuming nitric acids (IRFNAs) [nitric acid containing (di)nitrogen tetroxide, hydrogen fluoride (HF), and water] have been used as the U.S. Army's oxidizer of choice for many years in bipropellant rocket propulsion systems. Aluminum alloy tanks are used to store and transport IRFNA and also to store oxidizer in the missiles. HF in the liquid IRFNA is a very effective corrosion inhibitor reacting with the aluminum alloy to form a protective film. The majority of long-term storage data of IRFNA are with IRFNA containing HF.

Concern over the safety and handling of liquid IRFNA has generated an interest in gelled IRFNA with its improved safety characteristics. IRFNA gels currently being used are prepared by the addition of fine particles of silicon dioxide (SiO_2) to

Table 1 ICR from electrochemical studies and TACR from weight loss studies of 2014 Al alloy in IRFNA oxidizer media after specified immersion times

IRFNA oxidizer[a]	Cell code[b]	ICR, mg cm^{-2} day^{-1} [c]			TACR, mg cm^{-2} day^{-1}(60d[c])	
		25 days	60 days	100 days	Set A	Set B
		Nottingham				
Gel, CS, L	1 NLGAM(i)	0.043	0.0035	0.0015(93d)	0.100	0.113(29d)
	2 NLGAM(ii)	0.0466	0.0111	0.0018	—	—
	3 NLGAM(iii)	0.0084	0.0010	0.0006	—	—
Gel, A200 (3 wt%)	4 NGAM	~0.0205	~0.0641	0.0570(110d)	—	—
Gel, CS, L + P_4O_{10} (3 wt%)	5 NLGAM-3P(i)	0.0043	0.0002	≤0.0001	0.052	—
	6 NLGAM-3P(ii)	0.0044(23d)	—	—	—	—
Liquid + P_4O_{10}, 3 wt%	7 NAM-3P	≤0.0001(23d)	—	—	—	—
Liquid	8 NAM	—	0.0005	—	—	0.001(59d)
Gel, CS, L, +P_4O_{10} (0.5 wt%)	9 NLGAM-0.5P	—	—	—	—	0.004(59d)
		Huntsville				
Gel, A200(4.5)	HGAG	0.0004(12d)	—	0.0008(112d)	—	0.03(21d)
	HGAM	0.0012(14d)	—	0.0004(112d)	—	—
Gel, A200(4.5) + P_4O_{10}, 0.46 wt%	HGAG-0.5P	0.0009(14d)	0.0042(55d)	0.0009(112d)	—	—
	HGAM-0.5P	0.0013	0.0005(40d)	0.0002(113d)	—	—
Liquid	HAG	0.0006(14d)	0.0011(58d)	0.0013(114d)	—	—

[a]Oxidizer code: CS, 3 wt% Cab-o-sil (SiO_2); L, 28 wt% $LiNO_3$; A200(3), 3 wt% Aerosil 200 (SiO_2); A200(4.5), 4.5 wt% Aerosil 200.
[b]Cell code: N, Nottingham; H, Huntsville; L, 28 wt% $LiNO_3$; GA, gelled acid; A, liquid acid; M, metal; G, glass.
[c]Unless otherwise indicated.

act as the gellant. The SiO_2 is expected to react with the HF inhibitor to form silicon–fluorine or silicon–fluorine–oxygen compounds. The amount of silica necessary to form the gel is in excess of that required to react with the HF present, and the inhibiting characteristics of silicon–fluorine or silicon–fluorine–oxygen are unknown.

The corrosiveness of gelled IRFNA can be varied by the following approaches:

1) Modification by the addition of a corrosion inhibitor that does not react with the silica gelling agent.

2) Modification of the metal surface by pretreatment.

3) A combination of 1 and 2.

The methods and techniques discussed in Ref. 1 have been used to evaluate liquid and gelled IRFNA. The original work on liquid IRFNA was performed at the University of Nottingham as were the initial studies on gelled IRFNA.

The data reported and discussed in this article used approach 1, which adds an inhibitor to obtain a comparison with liquid IRFNA corrosion rates. Maximum long-term storage may require both prepassivation and the addition of an inhibitor.

These methods and techniques have been and are being used at present in a collaborative program between the University of Nottingham, UAH Propulsion Research Center, and MICOM Propulsion Directorate.

Experimental Results

Corrosion Data by Electrochemical Method—University of Nottingham

The electrochemical cells used in the University of Nottingham research contained a 2014 Al working electrode.[1] The data in Fig. 1 are typical of the data obtained from the first three cells (Table 1), which contained a lithium nitrate ($LiNO_3$) loaded IRFNA gel.

The E_{corr} values showed a sharp fall during the 12 h after each cell was set up. This was attributed to the breakdown of the air-formed oxide film on the aluminum surface. E_{corr} leveled off at ca. −650 mV. After ca. 10 days, E_{corr} rose slowly, leveling off at between −510 and −540 mV after 90 days. The steady increase in E_{corr} was attributed to the growth of a film of corrosion products on the metal surface.

The R_p values were steady at ca. 2 kΩ during the 10 days after each cell was set up. The R_p rose steadily during the next 80 days and leveled off in the range 80–150 kΩ. The R_p vs time curves were qualitatively similar to the E_{corr} vs time

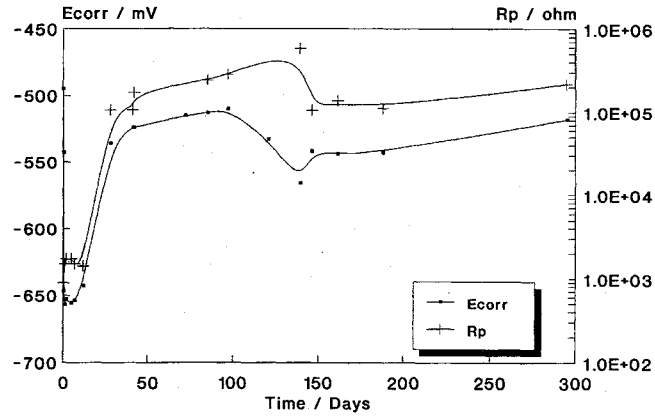

Fig. 1 Electrochemical data (cell 3).

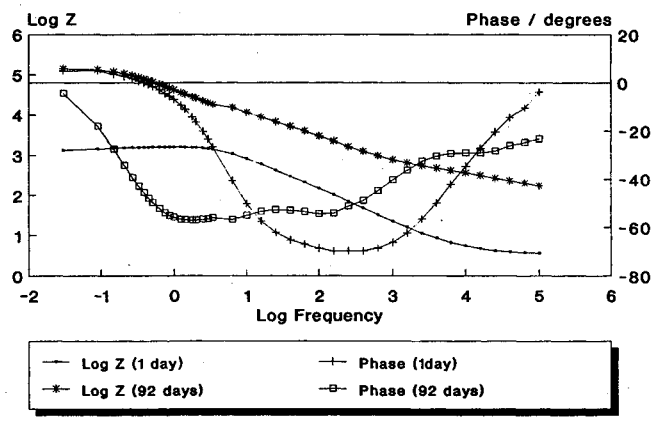

Fig. 2 Bode plots for cell 1 (1 and 92 days).

curves. A similar interpretation may be proposed. The R_p values recorded during the first 10 days were low, indicating a high corrosion rate. The corrosion rate slowed as a film of corrosion products was deposited on the metal surface.

The Bode plots obtained for cell 1 after 1 and 92 days were compared (Fig. 2). Three main time constants were observed in the impedance spectra:

1) A time constant at ca. 100 Hz, attributed to the oxide film on the metal surface.

2) An inductive feature at low frequencies, only evident on a Nyquist plot as an inductive loop.

3) A time constant at ca. 5 Hz, which appeared after 10 days immersion in gelled IRFNA, assigned to the corrosion product film.

Figure 3 shows the data for the cell that contains P_4O_{10} in the gel. The E_{corr} values fell steadily during the first 13 days after the cell was set up, to reach a minimum of −764 mV. E_{corr} then rose and had reached −485 mV after 105 days.

The R_p values measured for this cell remained steady in the range 4–20 kΩ during the first 13 days after the cell was set up. The R_p rose steadily after the first 13 days and an estimated R_p value of ca. 10 MΩ was obtained after 105 days. The initial fall in potential has been attributed to a stripping of the air-formed oxide film present on the metal surface. The subsequent rise in potential may be attributed to the formation of a protective layer of corrosion products.

The main difference between the cells without and with 3 wt% P_4O_{10} was the substantially higher R_p values reached by the latter. The steady-state R_p value for this cell was about two orders of magnitude higher. This implies that the equilibrium corrosion rate of 2014 Al in gelled IRFNA, containing 3 wt% P_4O_{10} is ca. 100 times lower than in gelled IRFNA. This apparent decrease in the corrosion rate may be attributed to a change in the corrosion product layer that forms after the initial air-formed oxide film has been stripped. The corrosion product layer in gelled IRFNA is assumed to be a mixture of AlF_3, Al_2O_3, and aluminum nitrate species. In gelled IRFNA containing 3 wt% P_4O_{10}, the layer is assumed to have incorporated some phosphate species, leading to a more resistive (and protective) film. The cell was monitored using the variation of the impedance spectrum with time as shown in Fig. 4. The impedance spectrum recorded after 1 day showed one main time constant at ca. 1 kHz. This has been assigned to the air-formed

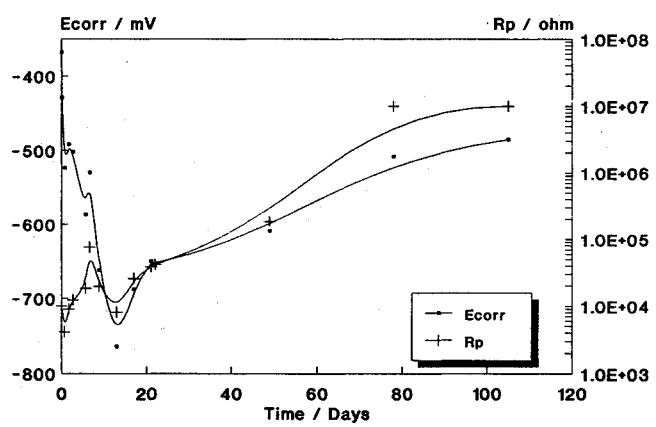

Fig. 3 Electrochemical data for cell 5 (P_4O_{10} additive).

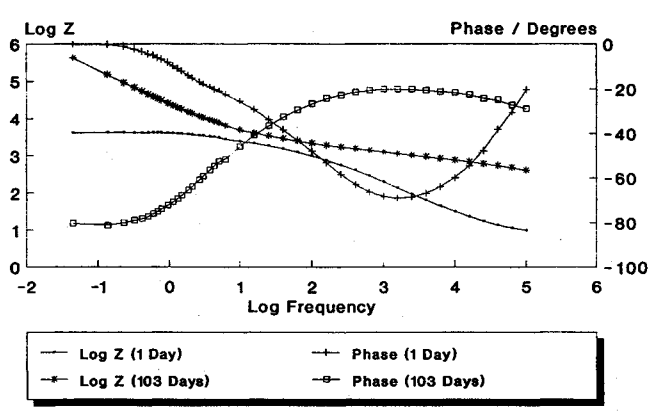

Fig. 4 Bode plots for cell 5 (1 and 103 days).

oxide present on the metal prior to immersion. The impedance spectrum recorded after 103 days showed one main time constant at ca. 0.1 Hz. This has been assigned to the corrosion product layer. There appeared to be no contribution to the measured impedance from the original oxide film.

This is in contrast to gelled IRFNA where a time constant assigned to the original oxide film was observed after 92 days. The gelled IRFNA containing 3 wt% P_4O_{10} appeared to have totally stripped the oxide film and replaced it with a highly resistive corrosion product layer.

The data on the cell containing IRFNA and P_4O_{10} show that during the first 10 days E_{corr} and R_p rose rapidly, from ca. −400 mV and 100 kΩ, respectively, and thereafter leveled off at ca. −180 mV and 6 MΩ, respectively. The rise in E_{corr} was indicative of a film-thickening process. The high values of E_{corr} and R_p after leveling off implied that the film was highly protective. The corrosion behavior of 2014 Al in IRFNA containing 3 wt% P_4O_{10} appears similar to that in gelled IRFNA containing 3 wt% P_4O_{10}, but in the absence of SiO_2 and $LiNO_3$, the protective film is established more rapidly. In both cases this film is likely to contain phosphate.

Corrosion Data by Electrochemical Method—University of Alabama in Huntsville

Data were taken with a cell identical to that used in the University of Nottingham research to check repeatability. The remainder of the experiments were conducted with the glass cells.[1]

The 2014 Al working electrode coupon of each glass cell was installed, as received, except for rinsing with 1,1,1-trichloroethane and drying in ambient air. No information on the previous history of these coupons was available and one side of some of them was covered with a black film. Optical microscopy showed them to possess a smooth surface, albeit with about 10% coverage by deposits, probably Al_2O_3. In contrast, the working electrodes of the BWE cells were carefully abraded with 600-grit emery before degreasing with 1,1,1-trichloroethane and drying in ambient air.

The data in Table 1 show that the glass and metal cells (HGAG and HGAM) behaved similarly during the 113 days reported. These data also show that two cells with added P_4O_{10} (HGAG-0.5P and HGAM-0.5P) behaved like the two cells without the added P_4O_{10}, giving the same low ICR values. The cell containing the liquid IRFNA (HAG) has a low ICR at 14 days and increases at 58 and 114 days. The rate at 14 days is consistent with the low values obtained with gelled IRFNA with and without P_4O_{10} and also with the low rates obtained with the liquid IRFNA cell (NAM) run at Nottingham and with the gel cell NLGAM(iii). However, gel cells NLGAM(i) and -(ii) have ICRs (10^{-3}), which are similar to that of cell HAG at 58 and 114 days. These 10^{-3} values are to be compared with the 10^{-4} values for the other gel cells discussed above.

The following general trends can be observed by evaluation of the data and experience gained during testing:

1) The liquid phase systems reach lower ICRs faster than the gelled systems. This occurs in liquids and gels with and without P_4O_{10}. A possible explanation for this is that the inhibitor concentration is greater in the liquids and it is free to diffuse to the aluminum at a faster rate.

2) The ICR decreases with leveling off after some period depending upon the system.

3) The ICRs for the liquid IRFNA and liquid IRFNA with P_4O_{10} and the gelled IRFNA with and without P_4O_{10} all level off at values with the same order of magnitude.

4) The long-term storability of the gelled IRFNA is comparable to the long-term storability of the liquid IRFNA.

5) Passivation of the aluminum prior to exposure to the oxidizer, IRFNA, will produce lower ICRs immediately.

Weight Loss

Figure 5 presents the time-average corrosion rate (TACR) data obtained from eight coupons in gelled IRFNA and eight

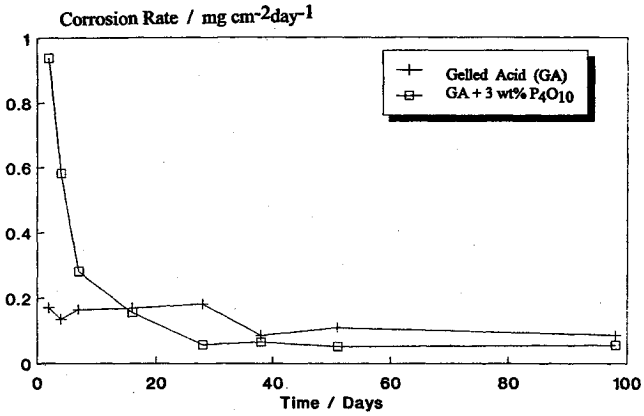

Fig. 5 Time-average corrosion rate vs time (set A).

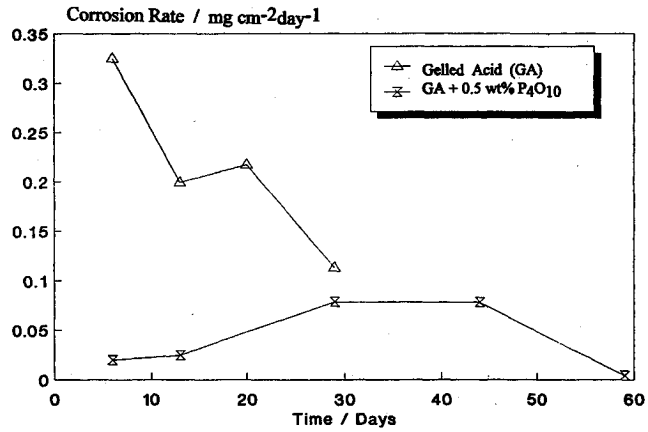

Fig. 6 Time-average corrosion rate vs time (set B).

coupons in gelled IRFNA containing 3 wt% P_4O_{10}. The coupons in gelled IRFNA undergo an initial TACR (ca. 0.15 mg cm^{-2} day^{-1}), which only decreases marginally, but steadily, to ca. 0.1 mg cm^{-2} day^{-1}. On the other hand the coupons in gelled IRFNA containing 3 wt% P_4O_{10} undergo a strikingly higher initial TACR (ca. 1 mg cm^{-2} day^{-1}), which, however, decreases rapidly, and after about 17 days is less than that in gelled IRFNA. After 98 days the TACR has fallen to ca. 0.06 mg cm^{-2} day^{-1}. The steady-state TACR of 2014 Al in gelled IRFNA was found to be approximately double the steady-state TACR in gelled IRFNA containing 3 wt% P_4O_{10}. This confirms the corrosion inhibiting effect of P_4O_{10} in gelled IRFNA. The P_4O_{10} is expected to be solvolyzed, yielding phosphoric acids in gelled IRFNA, and the inhibition is believed to arise from the formation of an aluminum phosphate film.

The formation of such a phosphate film could be preceded by the removal of the oxide film; this is indeed consistent with the exceptionally high initial TACR. The subsequent lower TACR values may then be seen as a consequence of the corrosion inhibiting effect of the phosphate film. This interpretation is consistent with the EIS study of cell NLGAM-3P(i).

Some further sets of eight coupons each were examined. The weight of the coupons that had been immersed in gelled IRFNA decreased steadily during the first 29 days of immersion. No results were obtained after 29 days because the numbers by which the coupons were identified had become obscured. The TACR decreased from ca. 0.3 mg cm^{-2} day^{-1} after 6 days to ca. 0.1 mg cm^{-2} day^{-1} after 29 days (Fig. 6). The TACR of the coupons that had been immersed in gelled IRFNA containing 0.5 wt% P_4O_{10} was steady at ca. 0.05 mg cm^{-2} day^{-1} during the 59 days of immersion (Fig. 6).

Coupons that had been immersed in liquid IRFNA showed no clear pattern of weight changes. Some of the samples showed a small weight gain and some a small weight loss. The average TACR was ca. 0.005 mg cm^{-2} day^{-1}. The corrosion inhibiting effect of P_4O_{10} in gelled IRFNA is confirmed by these results. However, the average TACR of 2014 Al in gelled IRFNA containing 0.5 wt% P_4O_{10} (Fig. 6) is ca. 10 times higher than the average TACR in IRFNA.

These data confirm the conclusion that in liquid IRFNA the high concentration of inhibitor (0.6%) easily diffuses to the surface of the metal and forms a protective film with corresponding low-corrosion rates. The corrosion rate is higher initially in the gel than in the liquid system, with most of the initial inhibitor (HF) reacted with the SiO_2 gellant and the added P_4O_{10}. Prepassivation of the metal surface will reduce this initial corrosion rate to the rate obtained in the liquid system.

Optical microscopic examination was performed on selected coupons used in the weight loss studies at a 200× magnification. No obvious signs of corrosion could be detected on blank (unimmersed) coupons, as expected. The rolling lines on the surface were clearly visible. Coupons that had been immersed in liquid IRFNA were covered with a thin film of corrosion products and the corrosion was uniform.

Two sets of coupons were evaluated that had been immersed in gelled IRFNA. The first set was immersed in IRFNA gel containing $LiNO_3$. After 60 days the coupons were pitted. Grain structure was detected in the bottom of the pits. The second set of coupons were immersed in gelled IRFNA without $LiNO_3$. After eight days the coupons differed little in appearance from the blanks, except for a pattern of small nuclei of an oxide film. After 21 days about 50% of the surface was covered by a deposit, but the underlying metal was unattacked. The corrosion rate calculated from the weight loss at 20 days was higher for the $LiNO_3$ loaded gel than for the unloaded gel (see Table 2).

Coupons that had been immersed in gelled IRFNA (CSL) containing 0.5 wt% P_4O_{10} for approximately 60 days were covered with a black film, largely removable by washing with water, and localized intergranular attack had also occurred.

Evaluation of the data in Table 1 provides some interesting information. First, for the TACR obtained with liquid IRFNA and for an IRFNA gel with $LiNO_3$ and 0.5 wt% P_4O_{10}, values of 10^{-3} were obtained after 59 days. Next, the liquid cell (HAG) at 58 days shows an ICR of 10^{-3} as did HGAG-0.5P with P_4O_{10}, but without $LiNO_3$ and NLGAM with $LiNO_3$ and without P_4O_{10}.

These results illustrate the difficulty in measuring corrosion rates. In certain cases the TACR and the ICR are similar and in other cases there are variations. Localized intergranular attacks with grains falling out of the surface (a mechanical process) can bring about a large weight loss for a relatively small amount of electrochemically measurable corrosion.

The data discussed previously suggest that when an inhibitor forms a uniform nonreactive layer on a metal, such as occurs with liquid IRFNA, a low corrosion rate is obtained. Pretreatment with a suitable reactant should passivate the surface with an even coat, thereby reducing total corrosion and pitting.

Surface Studies

Several of the aluminum 2014 blanks were polished and degreased. One blank was investigated using auger electron spec-

Table 2 Corrosion rates from weight loss experiments: 2014 Al coupons in IRFNA oxidizers

IRFNA oxidizer	Days	Corrosion rate mg cm^{-2} day^{-1}
Gel, A200 (4.5)	8	0.04
	21	0.03
Gel, CS, L	6	0.33
	20	0.22

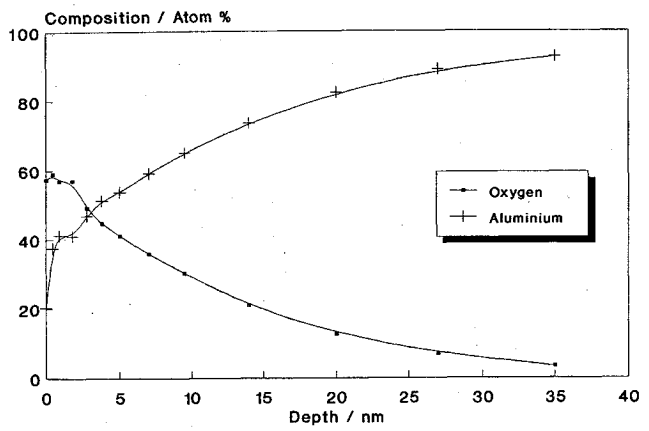

Fig. 7 Auger depth profile (2014 Al blank).

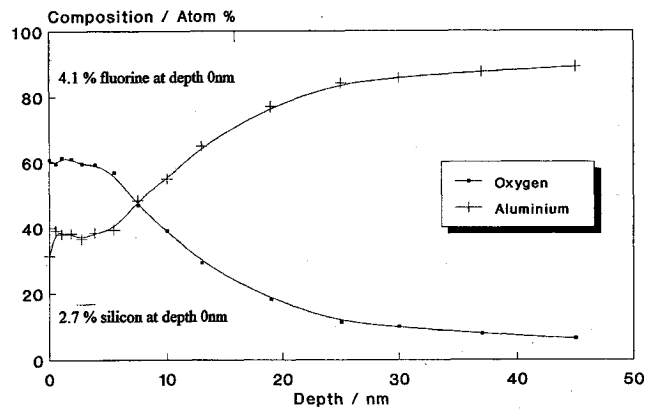

Fig. 8 Auger depth profile, sample (2014 Al) immersed in gelled IRFNA.

troscopy (AES) and one blank was studied using x-ray photoelectron spectroscopy (XPS).

The AES curves obtained are shown in Fig. 7. The two major components of the film on the metal surface are aluminum and oxygen. The other elements on the surface are Si, S, Cl, C, Ca, and Cu. The S, Cl, Cu, and C were largely confined to the surface of the film. These elements are presumed to be surface contamination obtained during handling, or from the degreasing process. Relatively low levels of Si and C persist throughout the film. These elements are assumed to be present as silicon carbide left over from the grinding process.

Copper detected in the subscale layers was expected since it is the main alloying element in 2014 aluminum. The Al-to-O ratio in the immediate subsurface layer is ca. 2:3. This indicates that the surface film is predominately Al_2O_3. The ratio increased with depth as successive layers of the film were ion-beam milled away. A measure of the oxide film thickness may be obtained from the depth at which the oxygen concentration falls to half its maximum value. As seen in Fig. 7, this thickness is 10 nm.

The XPS data are given in Table 3. Al, O, Si, C, F, and Mg were detected on the surface of the sample. The sample was subjected to 1–4 min of ion-beam milling. The concentration of F, C, Mg, and Si decreased after milling confirming that these elements were present largely as a result of surface contamination. This confirms the observations from the AES spectra. Peak binding energies were measured for the Al, Si, O, and F peaks on the unmilled surface. Two binding energies were obtained for the Al doublet. The lower binding energy (71.9 eV) is difficult to assign, however, it may arise from aluminum metal. The higher binding energy (74.2 eV) is probably assignable to Al_2O_3. The binding energy measured for Si (99.8 eV) was consistent with an organo–silicon complex.

Table 3 XPS data: 2014 Al coupon unimmersed (blank) surface composition/atom%

Milling time, min	C	O	Al	Si	F	Mg
0	23.6	37.9	23.6	11.7	2.0	1.3
1	18.0	36.0	31.6	10.1	1.1	1.3
4	6.8	41.6	37.3	10.0	0.8	0.8

Table 4 XPS data: 2014 Al coupon after immersion in gelled IRFNA (CS, L) at 25°C for 30 days and water washed surface composition/atom%

Milling time, min	C	O	Al	Si	F	N
0	25.2	46.2	13.5	6.2	4.5	4.5
1	9.9	46.1	24.9	12.8	5.2	0
4	10.6	42.8	27.9	14.1	3.0	0

This indicates that the silicon was derived from the contamination of the system with a silicon-containing oil or grease. The binding energy measured for O (531.8 eV) was consistent with Al_2O_3. The binding energy measured for F (684.9 eV) indicated the presence of metal fluoride on the surface presumably AlF_3, although the sample had not been exposed to any F-containing medium. The F-contamination of the surface could possibly have occurred by F being removed from other samples in the system by ion-beam milling.

The AES data from a 2014 aluminum coupon immersed in gelled IRFNA for eight days are shown in Fig. 8. The major components of the surface studied were Al and O. The other elements detected were N, Si, Cl, C, Ca, K, Cu, and F. The elements Cl, C, and K, which all occurred in very small concentrations, arise from contamination during handling. Copper, which was detected at a depth of 2.8 nm, is the major alloying component in the aluminum. Silicon was detected at a depth of >19 nm and is believed to be a residue of the polishing process. The Si, F, and N at the surface are all believed to be derived from the gelled acid. The presence of F on the surface suggests that not all of the HF in IRFNA is immobilized by the SiO_2 in the gelation process. The N was confined to the subsurface layers (1.1–2.8 nm). If this nitrogen is derived from gelled IRFNA, it is presumably deposited by nitrogen–oxygen species diffusing into the oxide film via cracks or flaws. The Al:O ratio increased steadily with increasing depth. At the immediate subsurface layer (0.6 nm) the ratio was ca. 2:3, indicating that the film was predominantly composed of Al_2O_3. The thickness of the oxide film was ca. 12.5 nm, indicating that the film had been thickened slightly in contact with gelled IRFNA.

The XPS data given in Table 4 were obtained on a coupon after storage for 30 days in gelled IRFNA. C, O, Al, Si, F, and N were detected on the metal surface. The sample was ion-beam milled for 1–4 min. The data in Table 4 show that the N was confined to the surface layer. The C, which decreased significantly after 1 min of milling was assumed to be a contaminant because of handling. The F content decrease with milling is consistent with the AES data showing that all of the HF from the IRFNA is not reacted/immobilized by the SiO_2 gellant. Peak binding energies were again measured for the unmilled surface. The Al (74.5 eV) and O (532.3 eV) peaks were attributed to Al_2O_3. The Si peak (100.4 eV) was assigned to an organo–silicon compound. The N peak (407.1 eV) was assigned to NO_3 and the F peak (685.4 eV) assigned to AlF_3.

The AES data shown in Fig. 9 are from a similar 2014 Al coupon immersed in gelled IRFNA with 0.5% P_4O_{10}. The sample surface was visibly coated with corrosion products, which were found to be distributed unevenly. It was impossible to select a truly representative area with the narrow Auger electron beam. The principal cationic component of the surface

Table 5 Huntsville XPS study

Coupon code	IRFNA oxidizer	Days immersed	F concentration/atom% at metal surface
2A6	None	0	0.63
2A3	Gel, A200 (4.5)	8	8.07
2A5	Gel, A200 (4.5)	21	13.75
HAG	Liquid	118	27.36

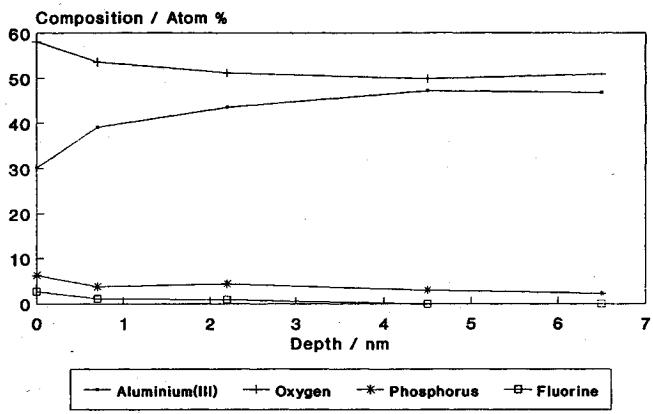

Fig. 9 Auger depth profile, sample (2014 Al) immersed in gelled IRFNA with P_4O_{10} additive.

was found to be Al(III) and significant amounts of the oxygen-binding elements, Si (10 atom%) and P (6.3 atom%), were observed. Oxygen (ca. 60 atom%) and fluorine (5.3 atom%) balanced the charges of these elements. The conclusions from the depth profile study were that silicon and fluorine were only significant in the surface, whereas phosphorus was still present down to 6.5 nm, the maximum depth examined. The thickness of the oxide layer, in the region selected for depth profiling, was in excess of 6.5 nm, since the oxygen content at this depth (50 atom%) had not decreased to half of its maximum value. These data indicate that the P_4O_{10} is reacting with the aluminum to form a passivation layer when added to the acid. Prepassivation of the aluminum tank with a phosphate solution should further enhance the passivation layer and increase the long-term storage of the IRFNA gel.

Table 5 compares XPS data obtained on Al coupons directed at understanding the extent of F uptake from liquid and gelled IRFNA. XPS general survey scans were carried out on the two coupons (coded 2A3 and 2A5) used in the weight loss study, a blank (unimmersed) coupon (coded 2A6) from the same batch and the coupon electrode, also from the same batch, recovered after dismantling the glass electrochemical cell that had contained liquid IRFNA for 118 days (HAG). The main purpose was to investigate the extent of fluorine uptake on to the coupon surface after immersion in the oxidizer media for the specified time periods. It was of particular interest to ascertain whether fluorine is still available to the metal surface from gelled IRFNA, since the SiO_2 gelling agent might be expected to take F^- out of circulation, so far as the metal is concerned, by the formation of Si–F linkages. The data demonstrate that this is not the case and that the extent of fluorine uptake by the alloy surface appears to be a function of immersion time in the gel, and the amount of F in solution.

Conclusions

The gels tested, with varying composition, reached the same low corrosion rates; i.e., showed the same suitability for long-term storage as the liquid IRFNA, but because of reduced concentration and/or low mobility of the inhibitor, it may take a longer time to establish the low rates.

The specific work discussed here shows that the rate of corrosion by the IRFNA decreases with time and levels off rather quickly because of the formation of a protective film on the surface of the aluminum.

The weight loss (TACR) data and the electrochemical (ICR) data are in agreement when pit corrosion is not present.

Surface studies have confirmed that a passivating film is formed on the aluminum surface that ensures a low corrosion rate and makes long-term storage possible.

Prior passivation of the aluminum surface provides protection to the surface, thereby reducing/eliminating the initial buildup of the protective film by the liquid/gel.

The combination of electrochemical corrosion rate data, weight loss data, and surface study data can provide very useful corrosion rates, corrosion mechanisms, and long-term storage data for metals in contact with corrosive materials.

The techniques and procedures are suitable for use in a variety of systems.

Acknowledgments

The authors extend their thanks to the U.S. Army for financial support under Contract DAJA 45-89-C-0022 through its European Research Office and for the supply of gelled IRFNA and 2014 Al; TRW for financial support under Contract FG7372DC3S and the supply of Al coupons; Krishnan Chittur, UAH Department of Chemical Engineering for his advice and guidance; Jeffrey Weimer, UAH Department of Chemistry and Department of Chemical and Materials Engineering for his assistance with the x-ray photoelectron spectroscopy investigations; and D. Thompson (MICOM, PD) for experimental assistance.

Reference

[1]Dove, M. F. A., Logan, N., Mauger, J. P., Allan, B. D., Arndt, R. E., and Hawk, C. W., "Laboratory Methodologies for Propellant Corrosion Research," *Journal of Propulsion and Power*, Vol. 12, No. 3, pp. 580–584.